

The Cell Perturbation Method for Turbulence Generation in Nested Large-Eddy Simulations for the Perdigão Field Campaign



Alex Connolly^{1*}, Fotini K. Chow¹ and Leendert Van Veen² *adac@berkeley.edu

AGU Fall Meeting 2019 A13N-3150

¹Department of Environmental Engineering, University of California Berkeley

²Department of Applied Mathematics, University of Twente

0 Abstract

Nested large-eddy simulations are not fed with turbulent flow fields by their parent mesoscale simulations. While turbulence will naturally develop in the large-eddy simulation, it can take prohibitively large fetches for this turbulence to develop (Mirocha *et al.* 2014). Here we test one method to ‘seed’ turbulence at the inflow boundary, the Cell Perturbation Method, or CPM (Muñoz *et al.* 2014). This method speeds the development of turbulence by perturbing the potential temperature field near the inflow boundary of a nested large-eddy simulation. In this work, the benefits of the CPM are evaluated in a real weather case over complex terrain relevant to the Perdigão project (Fernando *et al.* 2019).

1 Description of the Cell Perturbation Method

Perturbations applied to potential temperature along the inflow boundary

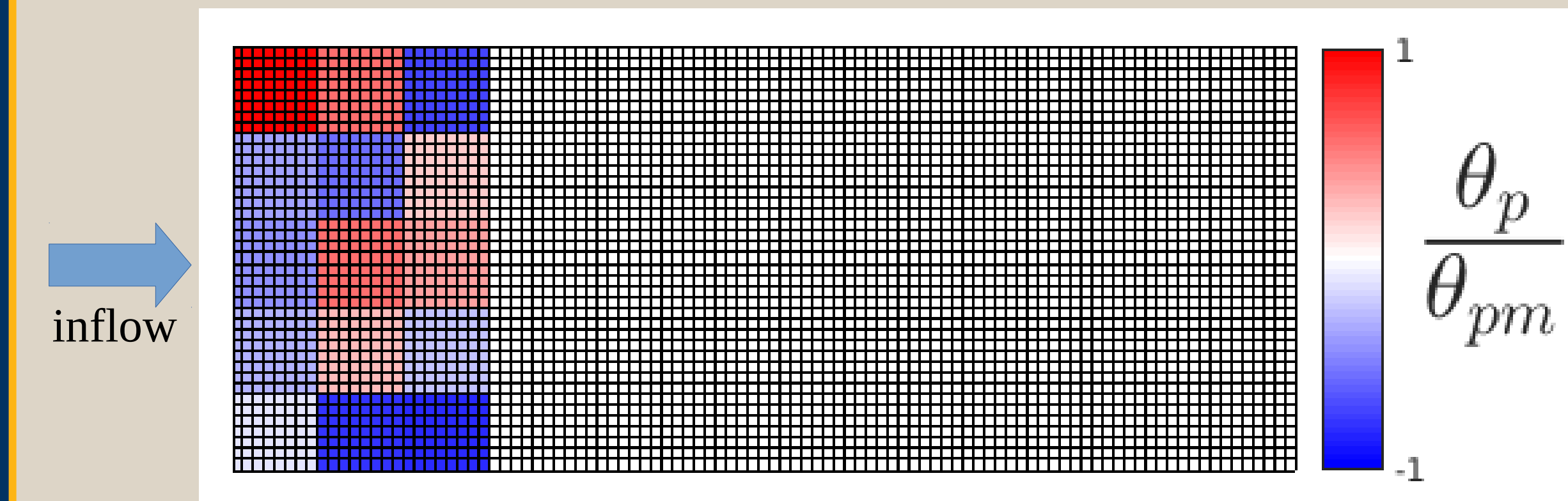


Fig. 1 Example CPM perturbations on single vertical level

- 3 cells of 8x8 grid points at each vertical level up to near boundary layer height
- Perturbation temperature, θ_p , drawn from uniform distribution in the range $[-\theta_{pm}, +\theta_{pm}]$ (Muñoz *et al.* 2014).
- Maximum perturbation magnitude calculated from a perturbation Eckert number, $Ec = 0.2$ (Muñoz *et al.* 2015)

$$Ec = U_g^2 / c_p \theta_{pm}$$

where U_g is the geostrophic wind, and $c_p = 1004.6 \text{ J kg}^{-1} \text{ K}^{-1}$ is the specific heat capacity of air.

2 Experimental Setup

CPM was implemented in the Weather Research and Forecasting (WRF) model version 3.9.1.1 developed by the National Center for Atmospheric Research (Skamarock *et al.* 2008).

Domain	d01	d02	d03_30s d03_30s_cpm	d03_3s d03_3s_cpm	d03 ref
$\Delta x = \Delta y$	6.75 km	2.25 km	150 m	150 m	150 m
$\Delta z_{min} - \Delta z_{max}$	21 m – 400 m	21 m – 400 m	21 m – 400 m	21 m – 400 m	21 m – 400 m
$N_x * N_y * N_z$	141 * 141 * 89	181 * 181 * 89	241 * 241 * 89	241 * 241 * 89	481 * 481 * 89
Δt [s]	30	10	0.5	0.5	0.5
Closure	MYNN	MYNN	TKE 1.5	TKE 1.5	TKE 1.5
Input Topography	2' – 4 km	30'' – 1 km	30'' – 1 km	3'' – 30 m	30'' – 1 km

- CPM applied only at the inflow boundary of d03_30s_cpm and d03_3s_cpm
- The d03 ref simulation has 240 extra points of fetch for resolved turbulence to develop
- Smaller d03 configurations are half the size of d03 ref, boundaries marked by the dashed gray line in Fig. 4c)
- Outermost domain, d01, is forced by the European Centre for Medium-range Forecast (ECMWF) data
- Inner simulations forced by a one-way nesting procedure

3 Effects of CPM on resolved turbulence

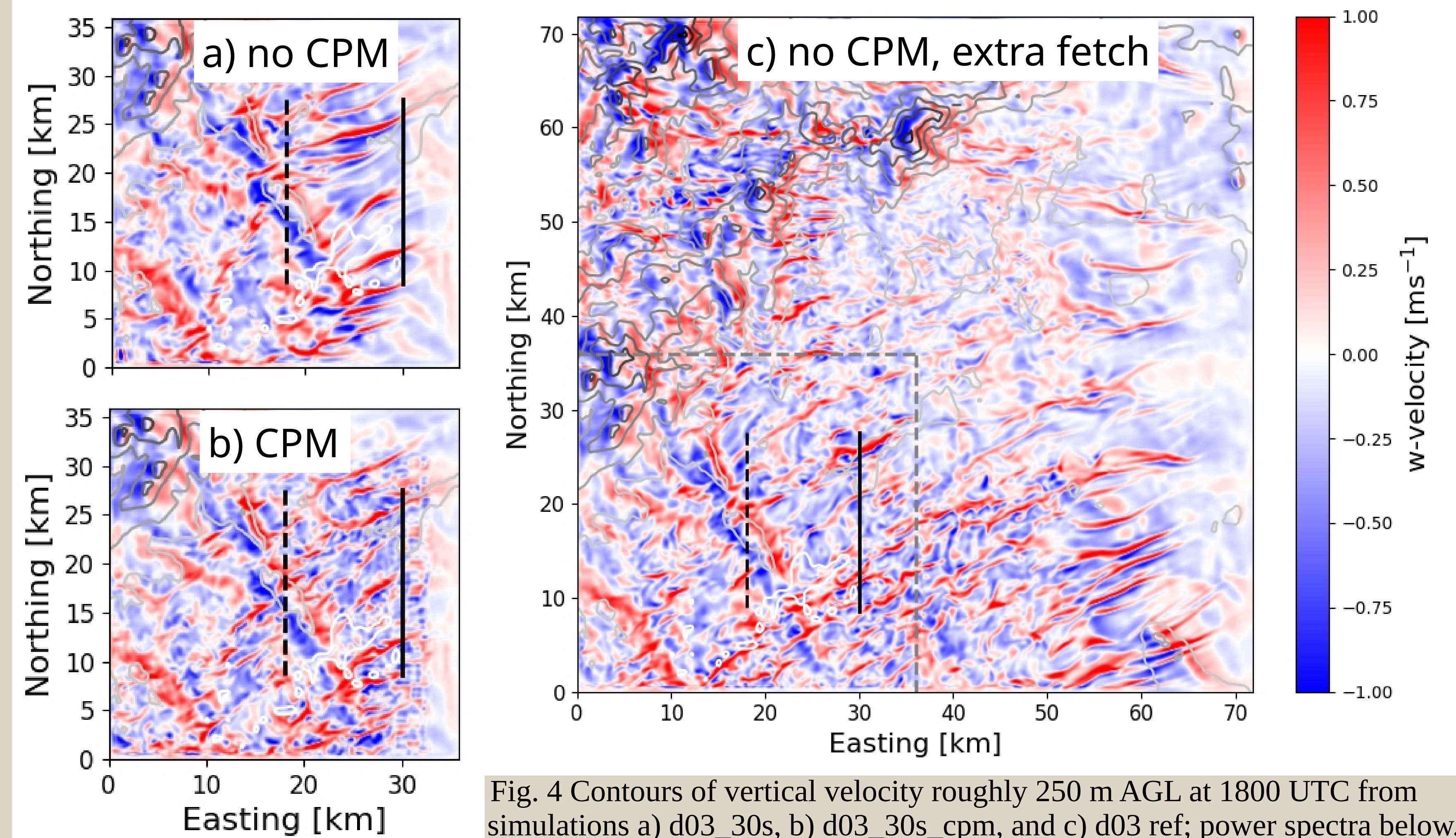
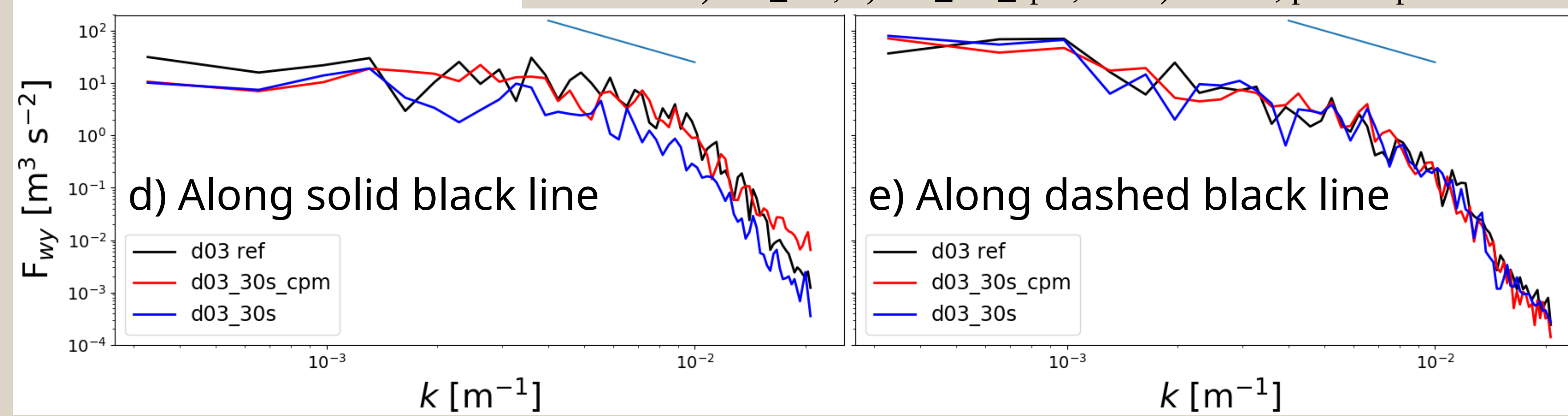


Fig. 4 Contours of vertical velocity roughly 250 m AGL at 1800 UTC from simulations a) d03_30s, b) d03_30s_cpm, and c) d03 ref; power spectra below.



4 Effects of topography resolution

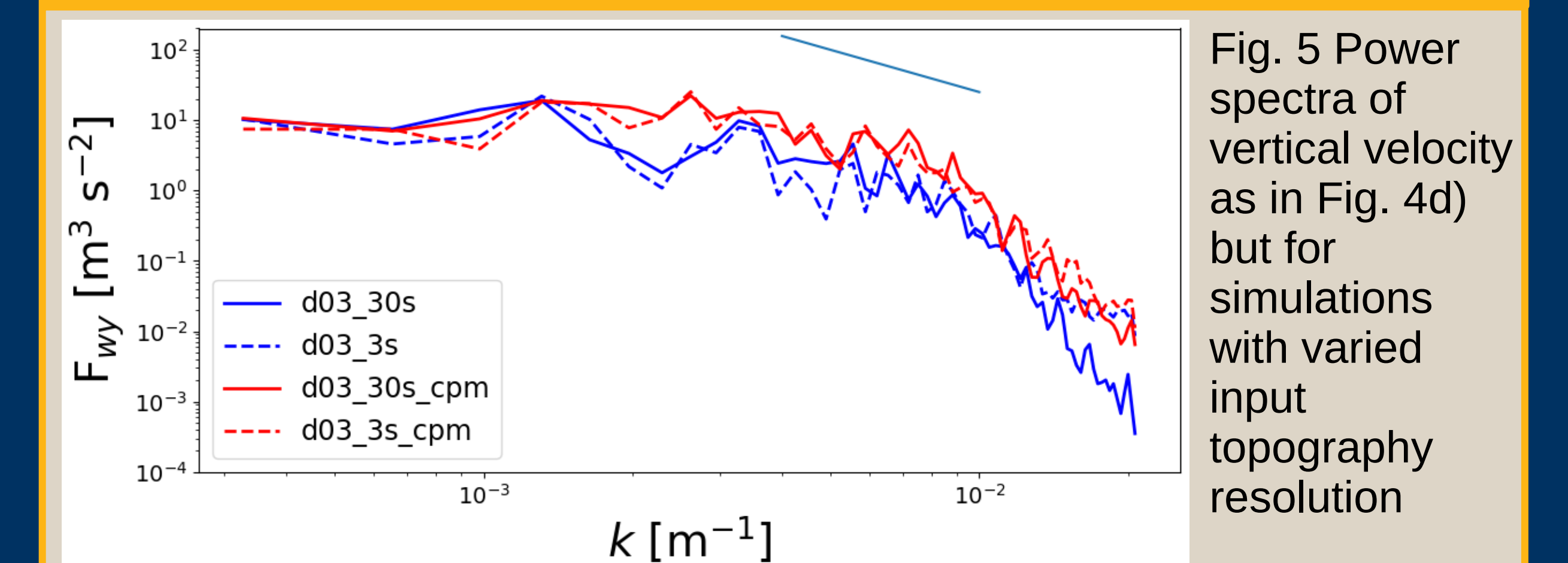


Fig. 5 Power spectra of vertical velocity as in Fig. 4d) but for simulations with varied input topography resolution

5 Conclusions

- The CPM leads to realistic turbulence spectra in the production and inertial ranges, even at short fetch as seen in Fig. 4d)
- At short fetch, the CPM may lead to increased energy at the highest wavenumbers, perhaps due to the perturbations themselves
- At long fetch, CPM does not lead to a different power spectrum than that seen in the reference domain with extra fetch as seen in Fig. 4e)
- Though finer resolved topography increases the turbulent energy, this effect may be isolated to the highest wavenumbers as seen in Fig. 5
- These results bode well for conducting multiscale simulations at less computation expensive because the CPM is cheaper than extra fetch.

Acknowledgments

We would like to acknowledge high-performance computing support from Cheyenne (doi:10.5065/D6RX99HX) provided by NCAR's Computational and Information Systems Laboratory, sponsored by the National Science Foundation.

Specific funding was provided by National Science Foundation grant AGS-1565483.

Special thanks to Prof. dr. ir. B.J. Geurts of the University of Twente and to James Neher of the University of California Berkeley.

References

- Fernando, H., and Coauthors, 2019: The Perdigão: Peering into microscale details of mountain winds. *Bulletin of the American Meteorological Society*, 100 (5), 799–819.
- Mirocha, J., B. Kosovič, and G. Kirkil, 2014: Resolved turbulence characteristics in large-eddy simulations nested within mesoscale simulations using the weather research and forecasting model. *Monthly Weather Review*, 142 (2), 806–831.
- Muñoz-Esparza, D., B. Kosovič, J. Mirocha, and J. van Beeck, 2014: Bridging the transition from mesoscale to microscale turbulence in numerical weather prediction models. *Boundary-layer meteorology*, 153 (3), 409–440.
- Muñoz-Esparza, D., B. Kosovič, J. Van Beeck, and J. Mirocha, 2015: A stochastic perturbation method to generate inflow turbulence in large-eddy simulation models: Application to neutrally stratified atmospheric boundary layers. *Physics of Fluids*, 27 (3), 035102.
- Skamarock, W. C., J. B. Klemp, J. Dudhia, D. O. Gill, D. M. Barker, W. Wang, and J. G. Powers, 2008: A description of the advanced research WRF version 3. Tech. rep., NCAR.

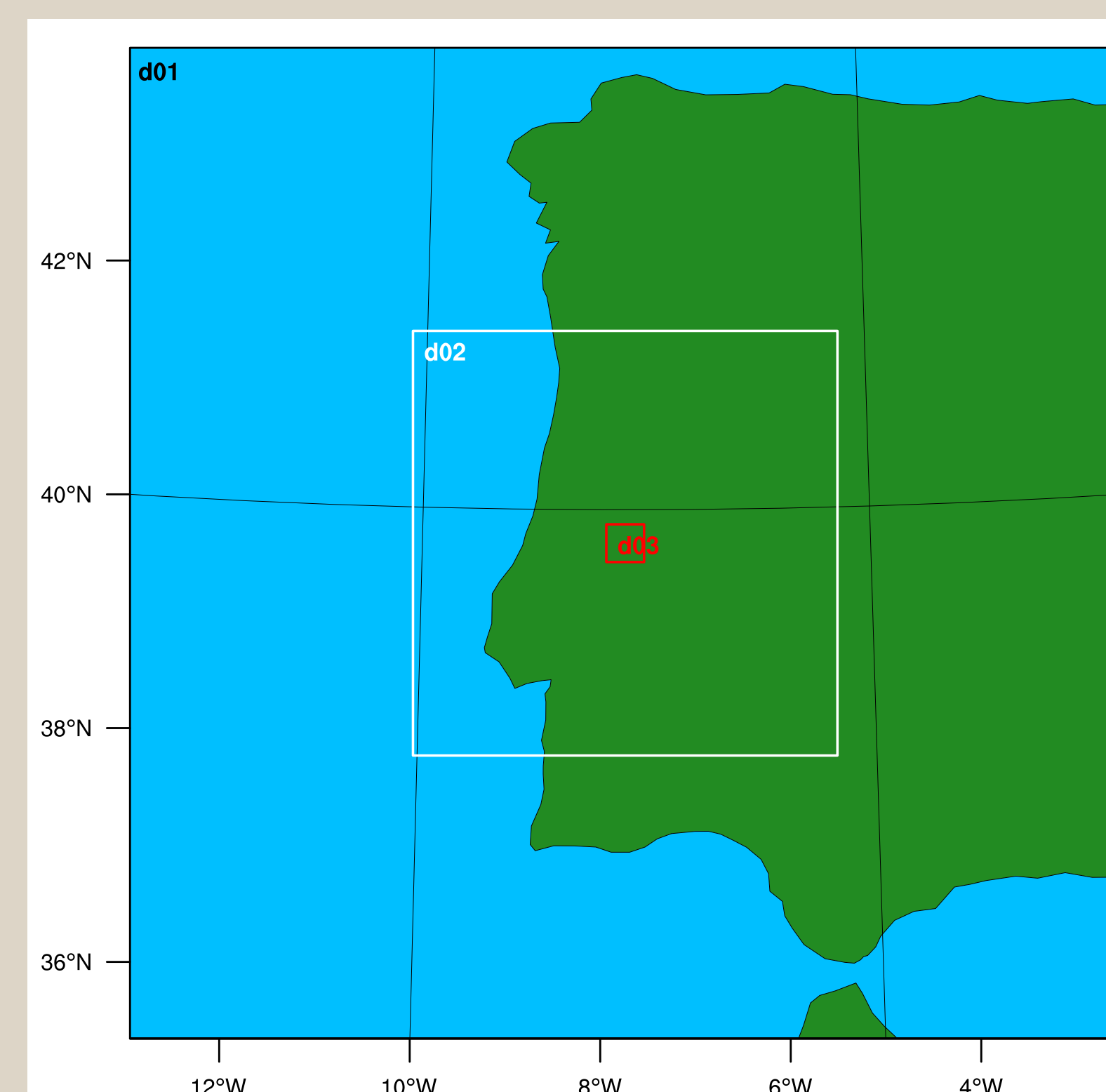


Fig. 2 Nested simulation domains used in WRF

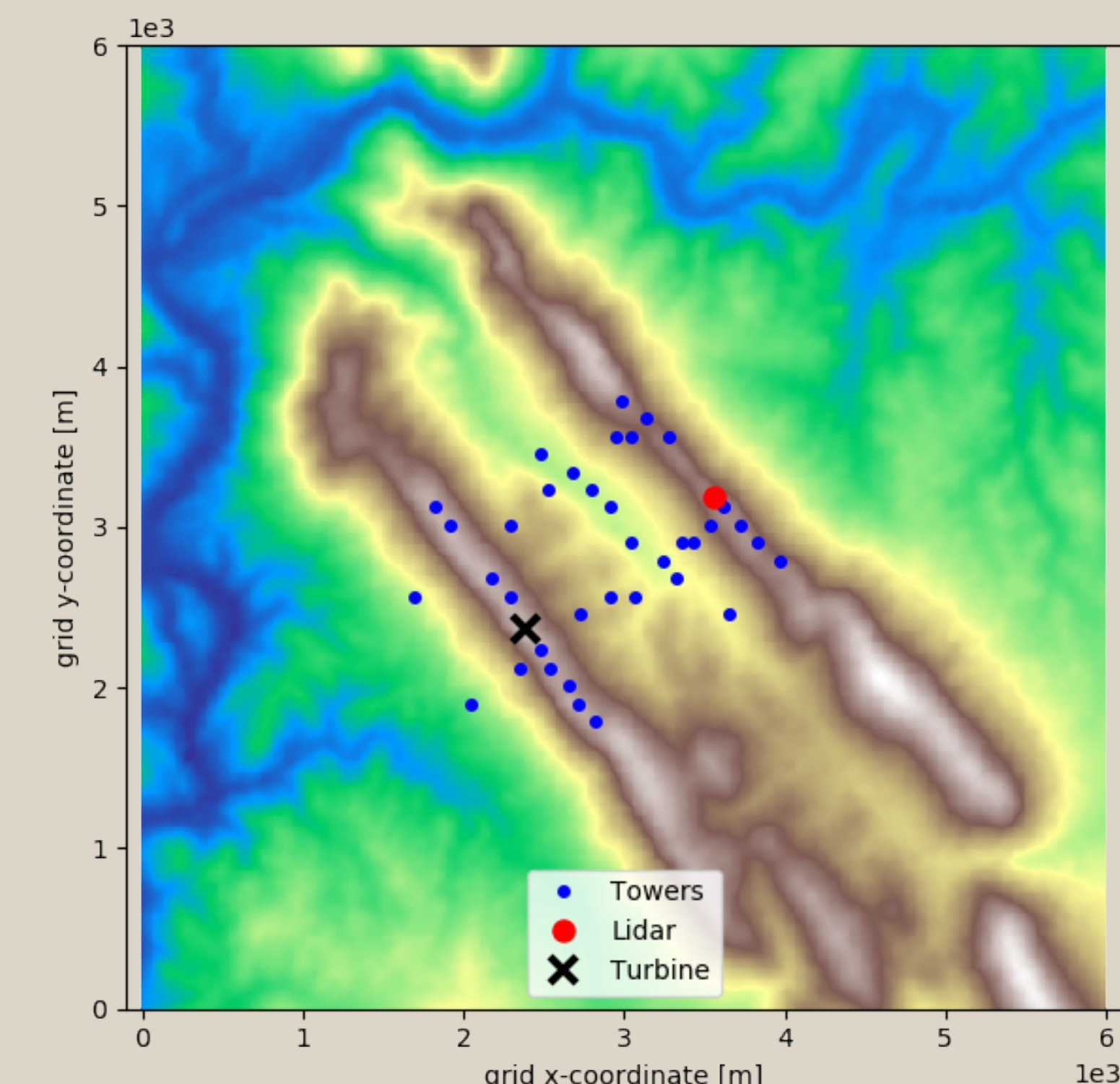


Fig. 3 Zoom in of Perdigão field site and instrumentation.